ACS Macro Letters

Letter

pubs.acs.org/macroletters

Influence of Molecular Solvation on the Conformation of Star Polymers

Xin Li,[†] Lionel Porcar,[‡] Luis E. Sánchez-Diáz,[†] Changwoo Do,[†] Yun Liu,[§,∥] Tae-Hwan Kim,[⊥] Gregory S. Smith,[†] William A. Hamilton,[#] Kunlun Hong,*[,○] and Wei-Ren Chen*[,†]

[†]Biology and Soft Matter Division, [#]Instrument and Source Division, and [○]Center for Nanophase Materials Sciences, Oak Ridge National Laboratory, Oak Ridge, Tennessee 37831, United States

[‡]Institut Laue-Langevin, B.P. 156, F-38042 Grenoble CEDEX 9, France

[§]The NIST Center for Neutron Research, National Institute of Standards and Technology, Gaithersburg, Maryland 20899-6100, United States

[∥]Department of Chemical Engineering, University of Delaware, Newark, Delaware 19716, United States

[⊥]Research Reactor Utilization Department, Korea Atomic Energy Research Institute, Daejeon 305-353, Korea

Supporting Information

ABSTRACT: We have used neutron scattering to investigate the influence of concentration on the conformation of a star polymer. By varying the contrast between the solvent and the isotopically labeled stars, we obtain the distributions of polymer and solvent within a star polymer from analysis of scattering data. A correlation between the local desolvation and the inward folding of star branches is discovered. From the perspective of thermodynamics, we find an analogy between the mechanism of polymer localization driven by solvent depletion and that of the hydrophobic collapse of polymers in solutions.

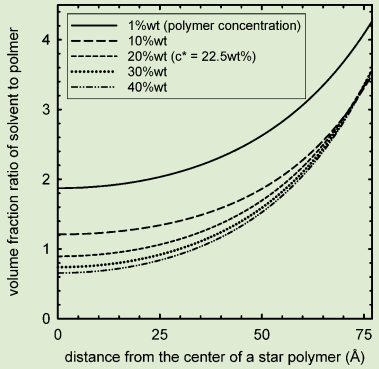

Star polymers are synthetic macromolecules consisting of linear polymer branches emanating from the molecular center.[1−4] They are characterized by the structural features of both linear polymers and hard colloids. There is wide interest in their properties because of their structural novelty as well as their role in a variety of industrial applications.[1,5] It is now an important family of soft matter.[4]

There has been much interest in understanding the conformational properties of an isolated star including the density profile, overall size, and scattering functions.[1−4,6−23] For each single polymer branch, the steric hindrance decreases steadily with the distance from the molecular center.[1] As a result, the intrastar polymer density shows a nonuniform distribution, which decreases from the center toward the periphery. Scaling criteria have been developed to categorize the intrastar spatial regions characterized by different conformational features.[1,4,10]

Considerable effort has also been devoted to investigating the manner in which the interstar interactions affect the individual star conformations due to their flexible molecular architecture. Particularly, the conformational dependence of a star on its concentration has been examined by scattering experiments.[17,19] Results suggest that while the global size of a star, in terms of the radius of gyration (R_G), essentially exhibits no concentration dependence when the concentration, c, is less than the overlap concentration c^*, R_G indeed decreases progressively when c is raised above c^*. However, what R_G reflects is the integrated information on the intrastar density profile.[24] The detailed conformational variation, which involves the relocation of the polymer components and invasive solvent within a star, cannot be directly obtained from this coarse-grained information. At present, it is still difficult to computationally simulate this concentration effect in which solvent and polymer are incorporated explicitly. Therefore, for star polymers the microscopic mechanism of concentration-driven conformational evolution remains to be explored. This challenge provides the main motivation for this study.

Small angle scattering techniques, including both neutron (SANS) and X-ray (SAXS), provide experimental tools to obtain the conformation of stars in solution because of their accessible nanoscale spatial resolution. When $c > c^*$, the local polymer density around the star periphery increases because of the interpenetrating polymer arms. As a result, if a star is fully protonated, the intrastar distribution of excess scattering length density (SLD) $\Delta\rho(r)$ of a strained star becomes more

Received: March 27, 2014
Accepted: April 29, 2014
Published: April 30, 2014

 © 2014 American Chemical Society dx.doi.org/10.1021/mz500182m | ACS Macro Lett. 2014, 3, 458−461

homogeneous (red curve) than that of its isolated state (blue curve). Therefore, for both SANS and SAXS, the interstar interpenetration inevitably leads to a significant loss of scattering contrast. This concentration effect on the scattering behavior is conceptualized in Figure 1a. However, this intrinsic

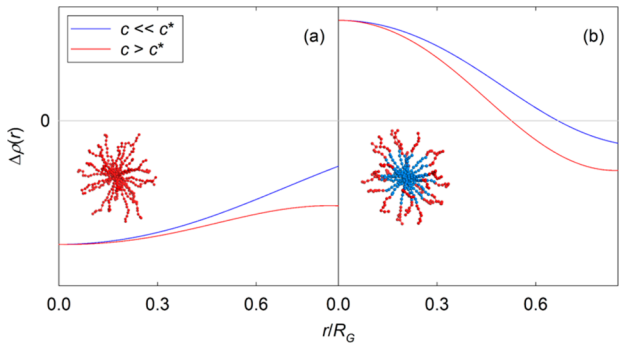

Figure 1. Schematic representation of the dependence of scattering contrast on concentration for (a) fully protonated star and (b) star with deuterated interior. $\Delta\rho(r)$ is the excess scattering length density (SLD) of a star in a deuterated solvent. The protonated and deuterated components of a star are represented by red and blue beads, respectively. The straight gray lines mark the SLD of deuterated solvent.

constraint can be bypassed by investigating a star with interior and periphery bearing the opposite isotopic label using SANS. Because the bound scattering lengths of a proton and a deuteron have opposite signs, the increase in the polymer density at the periphery in fact accentuates the SLD difference between the interior and that of periphery, as demonstrated in Figure 1b.

Therefore, in this report we investigate isotopically labeled polystyrene (PS) stars dissolved in a good solvent, tetrahydrofuran (THF), using SANS. THF solutions of fully protonated stars are investigated as a reference system. Both PS stars were synthesized at the Center for Nanophase Materials Sciences (CNMS), Oak Ridge National Laboratory (ORNL). The molecular weight determined from light scattering was found to be 538 k. The number of arms was found to be around 26. In the labeled stars, the protons residing in the interior of a star (around 60% of overall constituent protons according to SANS data analysis) are isotopically replaced by deuterons. The c^* of our system is estimated to be 22.5 wt % according to ref 16. More details of material synthesis are given in the Supporting Information (SI). The effect of isotopic labeling on the scattering signature of a star is clearly confirmed by the evolution of SANS intensity $I(Q)$ shown in the SI. Upon increasing the concentration, while an expected decrease in the $I(Q)$ for the fully protonated PS star is seen, the intensity of $I(Q)$ for the PS star with a deuterated core indeed increases continuously.

Since the flexible open architecture of the stars allow significant solvent penetration, we consider how this might affect the star conformation. For a SANS experiment the conformational information on a star is reflected by the zero-angle scattering $P(0)$,[24]

$$P(0) = nb_{\text{total}}^2 \tag{1}$$

where n is the number density of stars in THF and b_{total} is the sum of the bound scattering lengths of the constituent atoms of a single star. b_{total} can be explicitly expressed as

$$b_{\text{total}} = 4\pi \int_0^\infty \rho(r) r^2 \mathrm{d}r = 4\pi \int_0^\infty [\rho_{\text{polymer}}(r) + \rho_{\text{THF}}(\nu_{\text{THF}}(r) - 1)] r^2 \mathrm{d}r \tag{2}$$

where $\rho_{\text{polymer}}(r)$ and $\nu_{\text{THF}}(r)$ are the SLD distributions of polymer and volume fraction of invasive solvent within a star, respectively. ρ_{THF} is the SLD of THF. Combining eqs 1 and 2, $P(0)$ is found to take the following expression

$$P(0) = n(\Delta b_s \gamma - b_0)^2 \tag{3}$$

where Δb_s is the product of the SLD difference between the deuterated and protonated THF, and the volume of polymeric components. b_0 is the scattering power of a star immersed in fully protonated THF. γ is the solvent deuterium−hydrogen (D/H) volume fraction. By changing γ, one can alter $P(0)$ without affecting the star conformation. Therefore, this contrasting technique provides a probe to assess the structural inhomogeneity within a star. Figure 2 presents the experimental

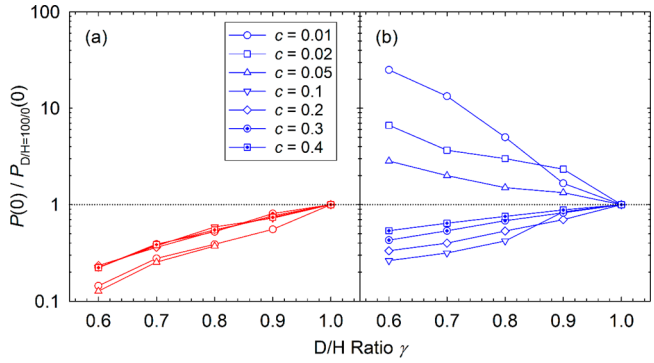

Figure 2. Normalized zero-angle scattering intensities of (a) fully protonated PS star and (b) deuterated-core PS star solutions in THF as a function of star weight fraction c at different D/H ratios X.

$P(0)$ for fully protonated and partially deuterated PS stars. Measurements of $P(0)$ obtained at different values of γ are normalized by that obtained in D_2O. The isotopic labeling is seen to influence the evolution of $P(0)$ significantly. By taking the derivative of eq 3, one finds

$$\frac{\mathrm{d}P(0)}{\mathrm{d}\gamma} = 2n\Delta b_s(\Delta b_s \gamma - b_0) \tag{4}$$

Since the bound scattering length of hydrogen is −3.8 fm, b_0 for a fully protonated star is a negligible positive number, which is more than an order of magnitude less than $\Delta b_s \gamma$ within the probed range of γ. Therefore, from eq 3 it is seen that the corresponding $P(0)$ increases monotonically with increasing γ. Moreover, as shown in Figure 2a, after normalization, the evolution of $P(0)$ essentially exhibits no concentration dependence when $c > 0.1$. This observation indicates that the possible conformational evolution is masked by the lack of scattering contrast. Meanwhile, since the bound scattering length of the deuteron is 6.5 fm, for partially deuterated star, b_0 and $\Delta b_s \gamma$ are of comparable magnitude. From eq 3, this means that a small conformational change can be amplified by SANS combining isotopic substitution of the star and contrast variation of the solvent. Indeed, upon increasing c, the occurrence of conformational variation and its close correlation

dx.doi.org/10.1021/mz500182m | ACS Macro Lett. 2014, 3, 458−461

with solvent penetration is qualitatively demonstrated by the characteristic variation of $(dP(0)/d\gamma)$ given in Figure 2b.

Having demonstrated the critical role solvent penetration plays in determining the star conformation, we develop a model scattering function to complement the experiment. Based on the aforementioned dense-core profile, the intrastar solvent and polymer distributions are explicitly parametrized in the form factor $P(Q)$ of a star. The SANS absolute intensity $I(Q)$ of concentrated star solutions not only contains the conformational information on a single star in the form factor $P(Q)$, but also that of the interstar spatial arrangement in the structure factor $S(Q)$. Since $I(Q)$ effectively can be factorized as the product of $P(Q)$ and $S(Q)$, the former can be effectively compartmentalized by normalizing the $I(Q)$ obtained at a certain γ to that obtained at $\gamma = 1$. One example of normalized $I(Q)$ is given in Figure 3. It contains the conformational

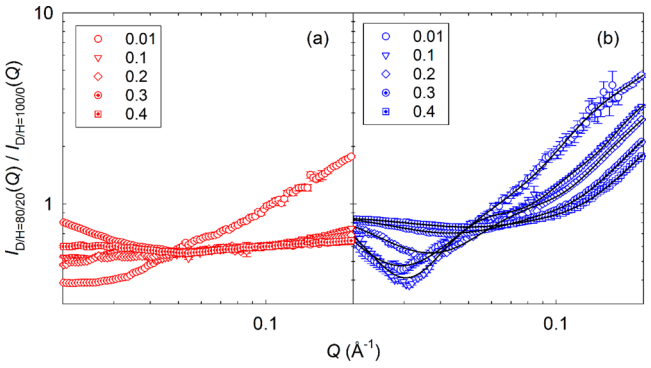

Figure 3. Normalized SANS absolute intensity $(I_{80/20}(Q)/ I_{100/0}(Q))$ of (a) a fully protonated PS star and (b) a PS star with deuterated core in THF solutions as a function of star weight fraction c. The black curves in (b) are the results of the theoretical model.

evolution of a single star with concentration. For fully protonated star solutions, the normalized $I(Q)$ (Figure 3a) is rather featureless. On the contrary, upon increasing c, the normalized $I(Q)$ for the partially deuterated star (Figure 3b) is seen to vary characteristically. The additional scattering features of Figure 3b, such as the locations of minima, originate from the core−shell SLD profile due to the isotopic substitution. They prove critical for extracting the conformational parameters and allow the determination of the distributions of solvent and polymer within a star separately and accurately. More details of model fitting are given in SI.

We summarize the main results of the star conformations obtained from SANS model fitting in Figure 4. Figure 4a gives the evolution of R_G as a function of c. R_G is seen to decrease continuously with increasing star concentration beyond c^*. A similar observation has also been reported previously in a different system.[17,19] To provide the physical origin of this size shrinkage, we evaluate the conformational evolution via scrutinizing the structural characteristics within the spatial resolution. In Figure 4b we present the radial density distributions of THF (red curves) and PS (blue curves) within a star deduced from our SANS fitting. Upon increasing c, the volume fraction of THF is seen to decrease continuously in the core region of 50 Å. Meanwhile, within the same region a progressive increase of PS density is also seen. From the ratio of the volume fraction of THF to that of PS presented in Figure 4c, denoted as $S(r)$, it is clearly seen that the average THF density is seen to decrease along the radial direction of a PS star. These two observations are correlated based on the following argument. From the perspective of interfacial free energy,[25,26] the free energy of the system is related to the solvent accessible surface area (SASA) of PS branches. Despite the difference in dimensionality, one can draw a direct connection between $S(r)$ and SASA. Because THF is a very good solvent for PS at room temperature, for an isolated PS star its branches are expected to be extended in THF. At high concentrations, the diminishing number density of THF in the vicinity of PS provides the driving force for the PS star to reduce its stretched branch entropically into a random coil-like conformation with lower free energy. As a result, an inward relocation of PS branches is triggered by the molecular desolvation. Therefore, the size shrinkage is a reflection of this conformational evolution occurring at the microscopic level. Meanwhile, upon increasing the concentration of PS stars in the solution, the degree of interstar interpenetration and congestion are expected to increase progressively. The enhancing physical contact among the PS components consequently causes the exodus of THF solvent. Therefore, the contribution of excluded volume effect to our experimental observation is also obvious. It is instructive to point out that the temperature-triggered hydrophobic collapse of polymers in aqueous solutions has also been attributed to the variation of local hydration level.[27,28] Our experimental finding suggests the relevance of solvent fluctuation in understanding the equilibrium configuration of general soft matter systems.

In conclusion, a close correlation between the molecular solvation and star conformation is revealed using SANS experiments. We provide the first experimental evidence of the detailed conformational dependence of a star polymer on concentration by combining isotopic substitution of the interior region of a star and isotopic contrast in the solvent. The progressive localization of star branches is triggered by the

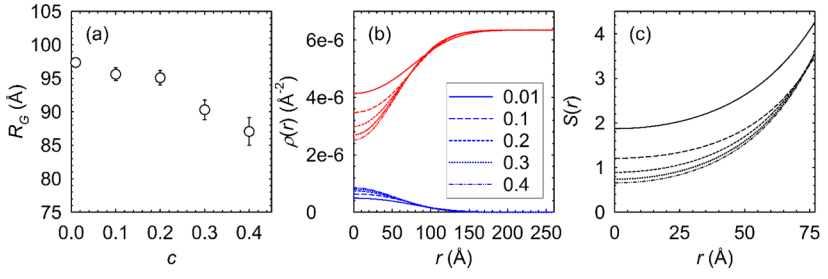

Figure 4. Conformational properties obtained from SANS model fitting: (a) R_G as a function of star concentration c in THF solutions; (b) The distributions of THF solvent (red curves) and PS components (blue curves) within a star at different c; (c) $S(r)$, the ratio of the volume fraction of THF to that of PS along the radial direction of star r.

dx.doi.org/10.1021/mz500182m | ACS Macro Lett. 2014, 3, 458−461

diminishing local solvent density and enhancing excluded volume effect. This conformational variation at the microscopic level is reflected by a size shrinkage at a mesoscopic length scale. We find an analogy between our observed mechanism, which controls the concentration-triggered conformational evolution, and that of the temperature-triggered hydrophobic collapse of a polymer in solution. This study suggests that the influence of solvent fluctuations on the structural variations may be a general property of soft matter systems.

■ ASSOCIATED CONTENT

Supporting Information

1. Synthesis of polystyrene star; 2. Small angle neutron scattering (SANS) experiment; 3. SANS data analysis. This material is available free of charge via the Internet at http://pubs.acs.org.

■ AUTHOR INFORMATION

Corresponding Authors

*E-mail: hongkq@ornl.gov.
*E-mail: chenw@ornl.gov.

Notes

The authors declare no competing financial interest.

■ ACKNOWLEDGMENTS

Research presented in this work is supported by the U.S. Department of Energy, Basic Energy Sciences, Materials Sciences and Energy Division. The EQSANS experiment at Oak Ridge National Laboratory's Spallation Neutron Source is supported by the Scientific User Facilities Division, Office of Basic Energy Sciences, U.S. Department of Energy. Synthesis of PS stars used in this research was conducted at the Center for Nanophase Materials Sciences, Oak Ridge National Laboratory, was sponsored by the Scientific User Facilities Division, Office of Basic Energy Sciences, U.S. Department of Energy. We acknowledge the support of the National Institute of Standards and Technology, U.S. Department of Commerce, in providing the neutron research facilities used in this work. We also greatly appreciate the support of SANS beamtime from ILL France and HANARO Korea.

■ REFERENCES

(1) Grest, G. S.; Fetters, L. J.; Huang, J. S.; Richter, D. *Adv. Chem. Phys.* **1996**, *94*, 67−163.
(2) Freire, J. J. *Adv. Polym. Sci.* **1999**, *143*, 35−112.
(3) Burchard, W. *Adv. Polym. Sci.* **1999**, *143*, 113−194.
(4) Likos, C. N. *Soft Matter* **2006**, *2*, 478−498.
(5) Inoue, K. *Prog. Polym. Sci.* **2000**, *25*, 453−571.
(6) Burchard, W. *Macromolecules* **1974**, *6*, 835−840.
(7) Burchard, W. *Macromolecules* **1974**, *6*, 841−846.
(8) Kajiwara, K.; Ribeiro, C. A. M. *Macromolecules* **1974**, *7*, 121−128.
(9) Mansfield, M. L.; Stockmayer, W. H. *Macromolecules* **1980**, *7*, 1713−1715.
(10) Daoud, M.; Cotton, J. P. *J. Phys. (Paris)* **1982**, *43*, 531−538.
(11) Witten, T. A.; Pincus, P. A.; Cates, M. E. *Europhys. Lett.* **1986**, *2*, 137−140.
(12) Witten, T. A.; Pincus, P. A. *Macromolecules* **1986**, *19*, 2509−2513.
(13) Grest, G. S.; Kremer, K.; Witten, T. A. *Macromolecules* **1987**, *20*, 1376−1383.
(14) Adam, M.; Fetters, L. J.; Graessley, W. W.; Witten, T. A. *Macromolecules* **1991**, *24*, 2434−2440.
(15) Dozier, W. D.; Huang, J. S.; Fetters, L. J. *Macromolecules* **1991**, *24*, 2810−2814.
(16) Willner, L.; Jucknischke, O.; Richter, D.; Farago, B.; Fetters, L. J.; Huang, J. S. *Europhys. Lett.* **1992**, *19*, 297−303.
(17) Richter, D.; Jucknischke, O.; Willner, L.; Fetters, L. J.; Lin, M.; Huang, J. S.; Roovers, J.; Toporowski, P. M.; Zhou, L.-L. *J. Phys. IV* **1993**, *3*, 3−12.
(18) Grest, G. S. *Macromolecules* **1994**, *27*, 3493−3500.
(19) Willner, L.; Jucknischke, O.; Richter, D.; Roovers, J.; Zhou, L.-L.; Toporowski, P. M.; Fetters, L. J.; Huang, J. S.; Lin, M. Y.; Hadjichristidis, N. *Macromolecules* **1994**, *27*, 3821−3829.
(20) Roovers, J.; Toporowski, P. M.; Douglas, J. *Macromolecules* **1995**, *28*, 7064−7070.
(21) Gast, A. P. *Langmuir* **1996**, *12*, 4060−4067.
(22) Shida, K.; Ohno, K.; Kimura, M.; Kawazoe, Y. *J. Chem. Phys.* **1996**, *105*, 8929−8936.
(23) Stellbrink, J.; Allgaier, J.; Monkenbusch, M.; Richter, D.; Lang, A.; Likos, C. N.; Watzlawek, M.; Löwen, H.; Ehlers, G.; Schleger, P. *Prog. Colloid Polym. Sci.* **2000**, *115*, 88−92.
(24) Feigin, L. A.; Svergun, D. I. *Structure Analysis by Small-Angle X-ray and Neutron Scattering*; Plenum Press: New York, 1987.
(25) Tanford, C. *Proc. Natl. Acad. Sci. U.S.A.* **1979**, *76*, 4175−4176.
(26) Tanford, C. *The Hydrophobic Effect: Formation of Micelles and Biological Membranes*, 2nd ed.; Wiley: New York, 1980.
(27) ten Wolde, P. R.; Chandler, D. *Proc. Natl. Acad. Sci. U.S.A.* **2002**, *99*, 6539−6543.
(28) Chandler, D. *Nature* **2005**, *437*, 640−647.